Bioorganic & Medicinal Chemistry 20 (2012) 5649–5657

Contents lists available at SciVerse ScienceDirect

Bioorganic & Medicinal Chemistry

journal homepage: www.elsevier.com/locate/bmc

Synthesis, biological evaluation, and molecular docking of *N*-{3-[3-(9-methyl-9*H*-carbazol-3-yl)-acryloyl]-phenyl}-benzamide/amide derivatives as xanthine oxidase and tyrosinase inhibitors

Babasaheb P. Bandgar [a,*], Laxman K. Adsul [a], Hemant V. Chavan [a], Sadanand N. Shringare [a], Balaji L. Korbad [a], Shivkumar S. Jalde [a], Shrikant V. Lonikar [a], Shivraj H. Nile [b], Amol L. Shirfule [c]

[a] Medicinal Chemistry Research Laboratory, School of Chemical Sciences, Solapur University, Solapur 413255, Maharashtra, India
[b] Biochemistry Research Laboratory, School of Life Sciences, S.R.T.M. University, Nanded 431606, Maharashtra, India
[c] Food and Drug Toxicology Research Centre, National Institute of Nutrition, Hyderabad 500 004, AP, India

ARTICLE INFO

Article history:
Received 5 April 2012
Revised 29 June 2012
Accepted 1 July 2012
Available online 10 July 2012

Keywords:
Carbazole
Benzamide
Xanthine oxidase
Tyrosinase
Molecular docking

ABSTRACT

Claisen–Schmidt condensation of 3-formyl-9-methylcarbazole with various amides of 3-aminoacetophenone afforded *N*-{3-[3-(9-methyl-9*H*-carbazol-3-yl)-acryloyl]-phenyl}-benzamide/amide derivatives. All compounds were investigated for their in vitro xanthine oxidase (XO), tyrosinase and melanin production inhibitory activity. Most of the target compounds had more potent XO inhibitory activity than the standard drug (IC_{50} = 4.3–5.6 μM). Interestingly, compound **7q** bearing cyclopropyl ring was found to be the most potent inhibitor of XO (IC_{50} = 4.3 μM). Molecular modelling study gave an insight into its binding modes with XO. Compounds **7a**, **7d**, **7e**, **7g**, and **7k** were found to be potent inhibitors of tyrosinase (IC_{50} = 14.01–17.52 μM). These results suggest the possible use of these compounds for the design and development of novel XO and tyrosinase inhibitors.

1. Introduction

Xanthine oxidase (XO) is generally recognized as the terminal enzyme of purine catabolism in man, catalyzing the hydroxylation of hypoxanthine to xanthine and xanthine to uric acid.[1] During this process, xanthine oxidase generates superoxide anions and H_2O_2, which in the presence of chelated iron are converted into highly reactive hydroxyl radicals.[2] These reactive oxygen species (ROS) are associated in various pathological events including inflammation, metabolic disorders, cellular aging, reperfusion damage, atherosclerosis, and carcinogenesis.[3] Gout and hyperuricemia are metabolic disorders associated with abnormal amount of uric acid in the body, resulting in the deposition of urate crystals in joints and kidneys, causing inflammation as well as gouty arthritis and nephrolithiosis.[4] In addition, hyperuricemia has become an independent risk of chronic kidney diseases and cardiovascular diseases.[5] XO can also oxidize synthetic purine drugs, such as anti-leukemic 6-mercapto purine with loss of their pharmacological properties.[6] Therefore selective inhibition of XO may result in a broad spectrum chemotherapy for gout, cancer, inflammation and oxidative damage.

Allopurinol (Fig. 1), a potent XO inhibitor with purine moiety has been used clinically for more than 40 years.[7] Unfortunately, it has been reported to be associated with an infrequent but severe hypersensitivity[8] by increasing the concentration of allopurinol metabolite in blood to the point where it is rendered toxic. Allopurinol and its actual metabolite, oxipurinol, are substrates for N-1 ribosyl derivatives forming phosphoribosyl transferases. Oxipurinol is also converted by uridine phosphorylase to the N-7 ribosyl derivatives. Therefore, novel non-purine alternatives to allopurinol with potent XO inhibitory activity with minimum side effects are in great demand. The first novel non-purine XO inhibitor, febuxostat (Fig. 1), has received the approval for the treatment of hyperuricemia in gout patients in USA and Europe.[9] This encouraged various research groups to search for non-purine derivatives. In this effort many research groups have synthesized the structurally diverse compounds such as 1,3-diaryl triazole,[10] 1-phenyl pyrazole derivatives (Fig. 1),[11] flavonoids (Fig. 1),[12] chalcones (Fig. 1),[13] 1-acetyl 3,5-diaryl 4,5-dihydro pyrazoles,[14] *N*-(1,3-diaryl-3-oxopropyl)amides (Fig. 1),[15] and curcumin (Fig. 1).[16]

On the other hand, tyrosinase which is also referred to as polyphenoloxidase (PPO), is most widely associated with the production of melanin for the protection of skin from solar radiation. However, this beneficial trait comes in hand with some severe vices and human maladies since the overproduction of melanin results in skin hyperpigmentation, characterized by age spots,

* Corresponding author. Tel./fax: +91 214 2351300.
E-mail address: bandgar_bp@yahoo.com (B.P. Bandgar).

0968-0896/$ - see front matter © 2012 Published by Elsevier Ltd.
http://dx.doi.org/10.1016/j.bmc.2012.07.001

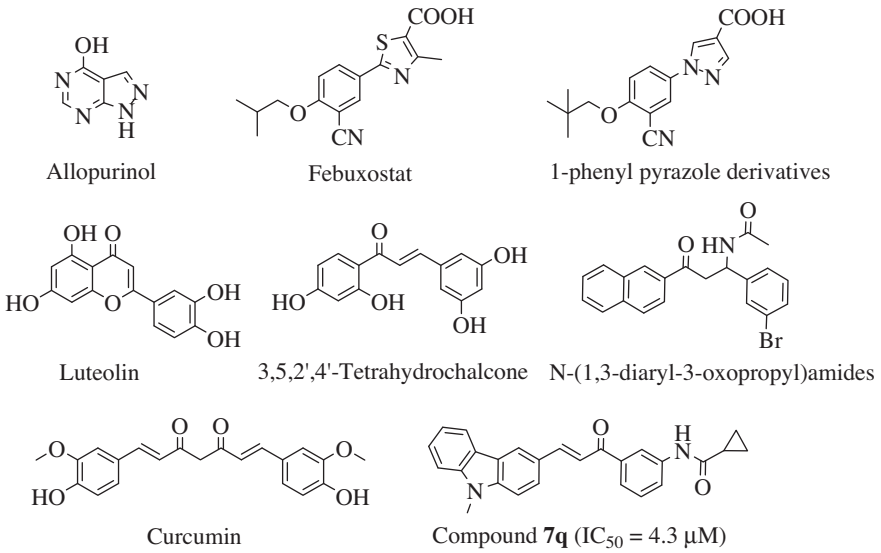

Figure 1. Some reported XO inhibitors and compound **7q**.

melasma and chloasama.[17] Melanin biosynthesis commences with two conversions catalyzed by tyrosinase, the hydroxylation of L-tyrosine to 3,4-dihydroxy phenyl L-alanine (L-DOPA) followed by the oxidation of L-DOPA to dopaquinone.[18] Quinones can polymerize non-enzymatically to melanin which is the most important natural biopolymer responsible of pigmentation and color patterns of mammalian skin.[19] The presence of oxidation products of L-tyrosine has recently been linked to the demise of neurons in several neurodenerative disorders such as Parkinson's and Huntington's diseases.[20] Although melanin production in human skin represents a primary defence mechanism against exposure to UV light, excessive accumulation of epidermal pigmentation can cause various disorders, such as, melasma, age spots, flecks, ephelide and sites of actinic damage. Therefore, tyrosinase inhibitors should be clinically useful for the treatment of some dermatological disorders associated with melanin hyper pigmentation and also important in cosmetics for whitening and depigmentation after sun burns. In addition, tyrosinase is responsible for undesired enzymatic browning of fruits and vegetables[21] that take place during senescence or damage at the post harvest handling, which makes the identification of novel tyrosinase inhibitors extremely important. Melanin synthesis in melanocytes by tyrosinase activity and catabolism of purine in presence of xanthine oxidase is accompanied by the generation of hydrogen peroxide, which, if inappropriately processed, can lead to the formation of hydroxyl radicals and other ROS. These highly reactive free radical compounds are potentially damaging to human tissues. For example, the hydroxyl radical ($HO^{\cdot}$), the superoxide anion radical ($O_2^{\cdot-}$), hydrogen peroxide (H_2O_2), and the peroxyl radical ($ROO^{\cdot}$) all have the capacity to generate metabolic products that could attack DNA or lipids in cell membranes. Therefore, the control of tyrosinase activity is of great importance in preventing the synthesis of melanin in the browning of fruits and vegetables and the accumulation of excessive level of epidermal pigmentation in animals.

Carbazole and its derivatives are the important class of heterocyclic compounds endowed with various pharmacological activities such as anti-cancer, antimicrobial, antiviral, anti-inflammatory and antioxidant activity.[22] Carbazole scaffold is present in many drugs such as carvedilol and carprofen. Carvedilol, an antihypertensive drug acts as a non-specific β-adrengic antagonist.[23] Carprofen, a non-steroidal anti-inflammatory drug (NSAID), is a selective COX-2 inhibitor.[24] More recently a series of phenylcarbazole molecules have been reported as antitumor agent,[25] Carbazole sulphonamides is a novel class of antimitotic agents against solid tumors.[26] But there were no reports on the synthesis and biological evaluation of *N*-{3-[3-(9-methyl-9*H*-carbazol-3-yl)-acryloyl]-phenyl}-benzamide/amide derivatives.

In an ongoing study on the design and synthesis of biologically active small molecules,[27] here we report the synthesis of *N*-{3-[3-(9-methyl-9*H*-carbazol-3-yl)-acryloyl]-phenyl}-benzamide/amide derivatives and describe these derivatives as potent XO and tyrosinase inhibitors. And we also investigated all the compounds for their inhibition of melanin production and cytotoxicity on B16F10 mouse melanoma cells.

2. Results and discussion

2.1. Chemistry

The target compounds were synthesized as shown in Scheme 1. Carbazole (**1**) on methylation with methyl iodide gave 9-methyl carbazole (**2**), which on Vilsmeier–Haack formylation gave 3-formyl-9-methylcarbazole (**3**). Commercially available 3-aminoacetophenone (**4**) was reacted with various acid chlorides (**5a**–**r**) in basic condition to obtain *N* (-3-acetyl-phenyl)-amides (**6a**–**r**). The 3-formyl-9-methylcarbazole (**3**) on Claisen-Schimdt condensation with various *N*-(-3-acetyl-phenyl)-amides (**6a**–**r**) in aqueous sodium hydroxide afforded target compounds (**7a**–**r**) in good to excellent yields. Similarly, 3-formyl-9-methylcarbazole (**3**) on Claisen-Schimdt condensation with 3-aminoacetophenone (**4**) in aqueous sodium hydroxide afforded the compound (**8**) in excellent yield (Scheme 2). All the synthesized compounds (**7a**–**r** and **8**) were characterized by IR, ^{1}H NMR, and MS. The IR spectrum of the compounds **7a**–**r** showed absorption due to –NH stretching at ~3350 cm^{-1}, amide carbonyl group at ~1670 cm^{-1} and α,β-unsaturated carbonyl group at ~1690 cm^{-1}. ^{1}H NMR spectrum (400 MHz) recorded in DMSO-d_6 showed a typical singlet at δ ~10.45 (for –NH) and a typical ^{1}H–^{1}H coupling constant in between 12 and 16 Hz showing *trans* stereochemistry of the double bond.

2.2. Inhibitory activity of xanthine oxidase (XO)

In this study, 19 newly synthesized carbazole derivatives were evaluated for their inhibitory activity against XO and the results are summarized in Table 1. In general, most of the target

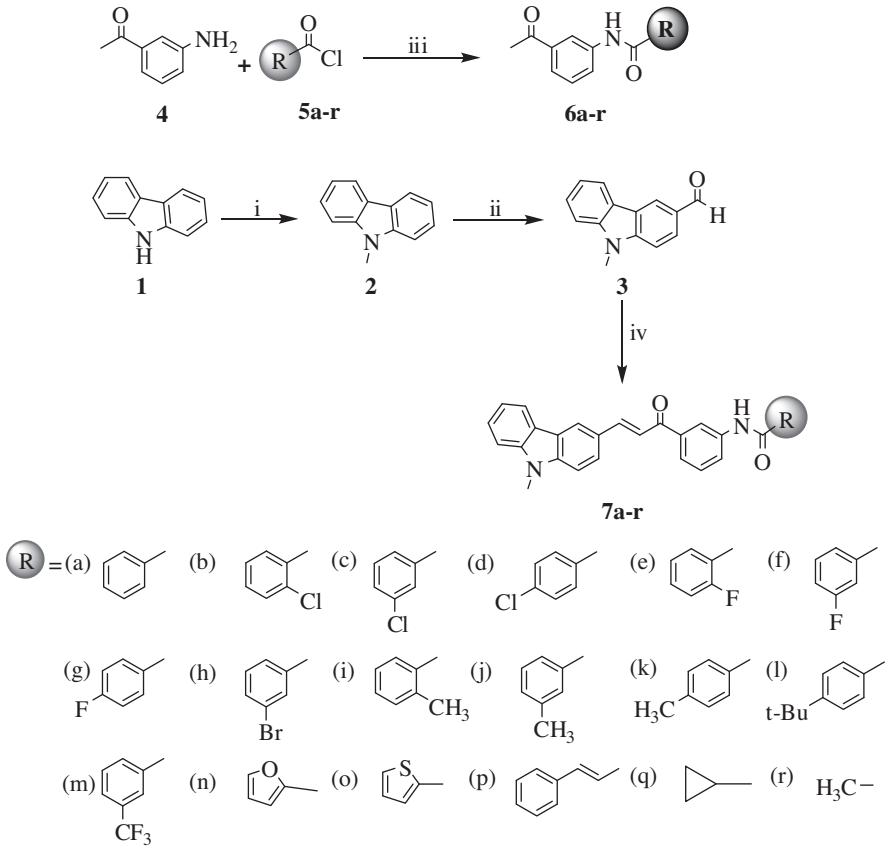

Scheme 1. Reagents and conditions:(i) DMF, NaH, CH_3I, rt, 3 h; (ii) DMF, $POCl_3$, 80 °C, 4 h; (iii) NaOH, rt; (iv) **6a–r**, NaOH, ethanol, rt, 24–36 h.

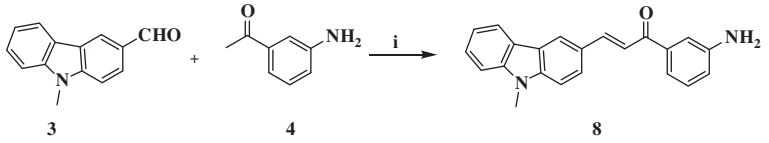

Scheme 2. Reagents and conditions: (i) NaOH, Ethanol, rt, 24 h.

compounds exhibited potent inhibitory activity against XO. Out of the 19 compounds screened, compounds **7c**, **7d**, **7f**, **7k**, **7m**, **7p**, and **7q** were found to be most active against XO with IC_{50} values ranging from 4.3 to 5.6 μM. The inhibitory activity of these compounds were comparable to that of allopurinol (IC_{50} = 8.5 μM). The concentration required to inhibit 50% XO (IC_{50}) was determined from the results of a series of concentrations tested. A lower IC_{50} value corresponds to a greater inhibitory activity. The intermediate compound **8** have showed the lower XO inhibitory activity similar to that of compound **7a**. The structure–activity relationship (SAR) study indicates that compounds with *meta* substituted amides have higher inhibitory activity than the *para* and *ortho* substituted amides with the exception of **7d** and **7k**. In general, electron withdrawing groups on amide ring have higher inhibitory activity than their counter parts containing electron donating groups with exception of **7k**. Replacement of aromatic amide ring by alicyclic ring that is, cyclopropyl (**7q**) gave the most active compound of the series with IC_{50} 4.3 μM. Increase in conjugation on amide side enhances the inhibitory activity; compound **7a** has weak inhibitory activity while compound **7p** has potent inhibitory activity. Position of substitution also influences inhibitory activity. Changing the position of fluorine/chlorine from *meta* (**7c** and **7f**) to *para* (**7d** and **7g**) decreases inhibitory activity. There is further decrease in inhibitory

Table 1
Xanthine oxidase inhibitory activity and docking score

Compound	XO inhibitory activity[a] IC_{50}(μM)	Docking score
7a	42.7 ± 2.74	–
7b	30.3 ± 1.23	–
7c	4.4 ± 0.89	75.249
7d	5.6 ± 1.03	72.721
7e	79.5 ± 3.12	–
7f	4.5 ± 0.89	74.978
7g	25.8 ± 1.56	–
7h	88.2 ± 3.12	–
7i	>100	–
7j	20.7 ± 1.45	–
7k	5.3 ± 2.13	78.874
7l	57.1 ± 3.65	–
7m	5.1 ± 2.0	–
7n	>100	–
7o	>100	–
7p	5.1 ± 1.30	75.234
7q	4.3 ± 0.89	74.481
7r	>100	–
8	48.5 ± 4.12	–
Allopurinol[b]	8.5 ± 2.13	63.174

[a] Values are the means of three experiments.
[b] Standard.

activity in *ortho* substituted compounds (**7b**, **7e** and **7i**). In addition, compound **7m** with trifluoromethyl group at *meta* position showed significant inhibition of XO.

2.3. Molecular modelling

To further understand the binding mode of synthesized compounds with XO, molecular docking studies of compounds **7c**, **7d**, **7f**, **7k**, **7p, and 7q** were performed using Accelrys. The docking of the compounds **7c**, **7d**, **7f**, **7k**, **7p**, **7q,** and Allopurinol has given the Dock score of 75.249, 72.721, 74.978, 78.874, 75.234, 74.481 and 63.174, respectively (Table 1). Docked conformation of ligands at active site of XO occupied the major amino acids as TRP283, LYS57, LYS57, THR79, ASP59, ARG793, SER307, SER344, VAL259, ARG793, SER306, TRP283, and ILE106. All the studied target molecules showed significant dock score and binding interactions as compared with the standard drug Allopurinol. The binding interactions of the target molecules and their representative binding sites are shown in Figure 2. The binding mode of **7c** to XO consists of amino acid residues, that are THR79, LYS57, and ASP59 (Fig. 2A) and for **7d** and **7f** are LYS57, ASP59 and ARG793 (Fig. 2B and C). The compound **7k** gets positioned in the cavity formed by LYS57, SER334, and SER307 (Fig. 2D). Compound 7**p** interacting with TRP283, SER307 and SER306 (Fig. 2E), while compound **7q** was with ASP59, VAL259 and TRP283 (Fig. 2F). The binding mode of these compounds explains the good potency of XO inhibition at the molecular level.

2.4. Inhibitory activity of tyrosinase

Tyrosinase inhibitory effects of the synthesized carbazole derivatives were tested on mushroom tyrosinase for both monophenolase and diphenolases activity. The activities were compared to that of kojic acid as positive inhibitor. The results of tyrosinase inhibition by the target compounds are summarized in Table 2. Out of the 19 synthesized compounds, compounds **7a, 7d, 7e, 7g,** and **7k** have shown potent tyrosinase inhibition with an IC_{50} value similar to that of kojic acid. The most active compound of the series is **7a** with an IC_{50} value 14.01 and 15.15 μM. The compound **8** have showed the minimum activity against tyrosinase. The SAR study indicate that electron withdrawing substituent on amide ring have higher inhibitory activity than their counterpart with electron donating group with the exception of **7k**. The bioisosteric replacement of aromatic ring of amide by heterocyclic ring, in particular thiophene and furan, results in 4- to 5-fold decrease in inhibitory activity. Similar replacement of aromatic amide ring by alicyclic cyclopropyl ring resulted in 5- to 6-fold decrease in inhibitory activity. In general *para* substituted compounds have highest inhibitory activity than *meta* and *ortho* substituent with the exception of compound **7e**. The introduction of conjugation in the active compound (**7a**) decreased the inhibitory activity (**7p**).

Among all the tested compounds, compound **7a** showed highest tyrosinase inhibitory activity and hence, we carried out the steady state kinetic analysis of compound **7a** for tyrosinase inhibition with respect to L-DOPA as substrate (S). A Lineweaver–Burk plot for inhibition of tyrosinase by compound **7a** was obtained with variable concentrations of **7a** and the substrate (Fig. 3). The interaction of lines indicated that compound **7a** was a competitive inhibitor of tyrosinase with respect to L-DOPA as a substrate, with a K_i value of 11.8 μM.

2.5. Melanin production inhibition and cytotoxicity

The inhibitory effects of the synthesized compounds were also examined on melanin production and their cytotoxicity on B16F10 mouse melanoma cells at concentrations of 20 μg/ml. The results of melanin production inhibition and cytotoxicity by the target compounds are summarized in Table 2. Compounds **7a** and **7g** inhibited melanin production by 42.5% and 40.5%, respectively, at concentrations of 20 μg/ml. Whereas, **7c**, **7d**, **7m** and **7q** have shown moderate inhibition of melanin production. However, inhibitions by these compounds may be appeared due their cytotoxic effects. On the other hand, cytotoxicity study revealed that almost all compounds were less toxic (80% melanoma cells survived) at 20 μg/ml except compound **7b** and **7i**. In terms of cytotoxicity and melanin production inhibition, compounds **7l**, **7n** and **7o** were best, showing melanoma cell survival up to 82.1–86.0% and melanin production inhibition up to 10.7–12.8% at 20 μg/ml.

3. Conclusion

We have synthesized and evaluated the carbazole derivatives for their in vitro xanthine oxidase, and tyrosinase inhibitory activity. And also synthesised compounds were examined for melanin production inhibition and cytotoxicity on B16F10 mouse melanoma cells. **7c**, **7d**, **7f**, **7k**, **7m**, **7p**, and **7q** were found to be most active against XO with IC_{50} values ranging from 4.3 to 5.6 μM. Compound **7q** was the most active compound of the series with IC_{50} 4.3 μM. Compounds **7a, 7d, 7e, 7g,** and **7k** have shown potent tyrosinase inhibition. The most active compound of the series is **7a** showing potent tyrosinase inhibition with an IC_{50} value 14.01 and 15.15 μM. Compounds **7l**, **7n** and **7o** were found to be best, showing melanoma cell survival up to 82.1–86.0% and melanin production inhibition up to 10.7–12.8%. Furthermore, Molecular docking was further performed to study the XO inhibitory activity; it was found that several interactions with the various amino acid residues in the binding site of XO might play a crucial role in its XO inhibitory activity. All these data suggested that these compounds might serve as candidates for the treatment of XO and tyrosinase based disorders and as lead compounds for further designing of new potential inhibitors of XO and tyrosinase.

4. Experimental

4.1. General

Melting points were recorded in open capillaries with electrical melting point apparatus and were uncorrected. IR spectra (KBr disks) were recorded using a Perkin–Elmer 237 spectrophotometer. ^{1}H NMR (400 MHz) spectra were recorded on a Bruker Avance spectrometer using DMSO-d_6 as solvent. Mass spectra were recorded on a Shimadzu LCMS-QP 1000 EX. All the reagents and solvents used were of analytical grade and were used as supplied unless otherwise stated. TLC was performed on silica gel coated plates for monitoring the reactions.

4.2. Synthesis of 3-formyl-9-methyl carbazole (3)

9-Methyl carbazole **2** (1.81 g, 10 mmol) was dissolved in dry DMF (20 ml) under anhydrous condition. It was cooled to 0 °C, $POCl_3$ (1.87 ml) was added drop wise for 30 min and stirring continued for 4 h at 80 °C. After completion of reaction (TLC), the reaction mass was poured over crushed ice (50 g), basified with NaOH, extracted with chloroform and dried over anhydrous Na_2SO_4. Organic layer was concentrated and purified through silica gel column using chloroform as eluting solvent to yield product **3** (1.15 g). Yield: 55%; off white solid; mp: 76–78 °C; IR (cm^{-1}): 3035, 2704, 1685, 1626, 1591, 1570, 1050, 750; ^{1}H NMR (300 MHz, DMSO-d_6, δ in ppm): 3.91 (s, 3H, NCH_3), 7.35 (t, 1H, J = 8.2 Hz, ArH), 7.40–7.60 (m, 3H, ArH), 7.98 (d, 1H, J = 8.2 Hz,

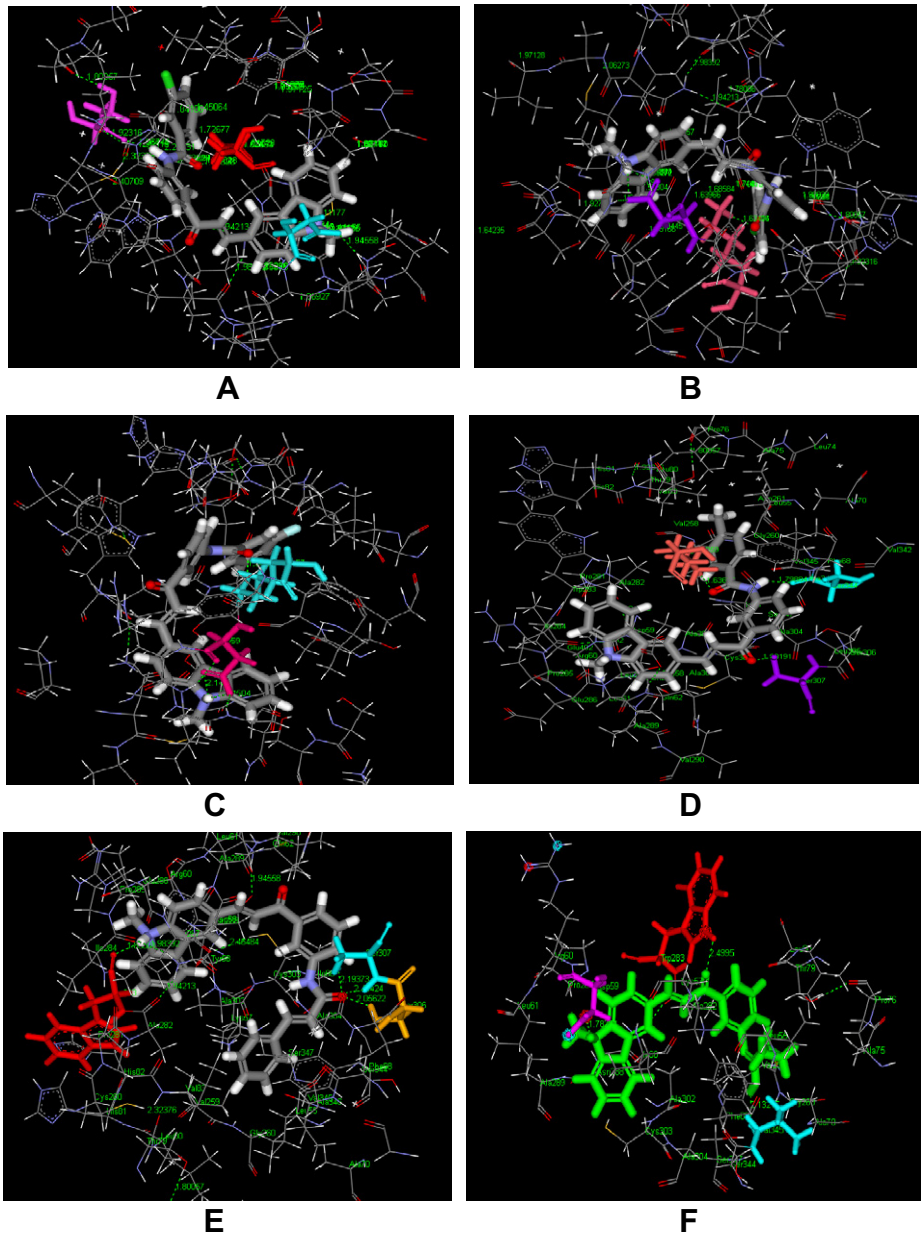

Figure 2. Molecular model of target compounds binding to active site of XO. Three dimensional models superimposed with **7c** (A), **7d** (B), **7f** (C), **7k** (D), **7p** (E) and **7q** (F).

ArH), 8.17 (d, 1H, J = 8.2 Hz, ArH), 8.60 (s, 1H, ArH), 10.10 (s, 1H, –CHO); m/z = 209.85 (m+1).

4.3. Synthesis of *N*-{3-[3-(9-methyl-9*H*-carbazol-3-yl)-acryloyl]-phenyl}-benzamide/amide derivatives (7a–r)

Amides **6a–r** (1 mmol) were dissolved in ethanol (15 ml), 1 ml 20% NaOH solution was added to it and stirred for 10 min at room temperature. Then, 3-formyl-9-methylcarbazole **3** (1 mmol) was added and stirring continued for 24 h at room temperature. After completion of reaction (TLC), reaction mixture was poured over crushed ice and stirred. The precipitate obtained was filtered and recrystallized by using methanol to obtain the target compounds (**7a–r**).

The physical and spectroscopic data of newly synthesized compounds are provided below.

4.3.1. *N*-{3-[3-(9-methyl-9*H*-carbazol-3-yl)-acryloyl]-phenyl}-benzamide (7a)

Yield 88%; Mp: 196–198 °C; IR (KBr, cm^{-1}): 3303, 2962, 2851, 1655, 1592,1462, 1255, 1106, 1019, 791, 708; ^{1}H NMR (400 MHz, DMSO-d_6, δ in ppm): 3.94 (s, 3H, NCH_3), 7.28 (t, 1H, J = 8.0 Hz, ArH), 7.42–7.78 (m, 7H, ArH and CH=CH), 7.88–8.10 (m, 6H, ArH and CH=CH), 8.12 (d, 1H, J = 8.0 Hz, ArH), 8.22 (d, 1H, J = 8.0 Hz, ArH), 8.44 (s, 1H, ArH), 8.75 (s, 1H, ArH), 10.53 (s, 1H, NH); m/z = 431.35 (m+1).

4.3.2. 2-Chloro-*N*-{3-[3-(9-methyl-9*H*-carbazol-3-yl)-acryloyl]-phenyl}-benzamide (7b)

Yield 80%; Mp: 120–122 °C; IR (KBr, cm^{-1}): 3303, 2962, 2851, 1655, 1592,1462, 1255, 1106, 1019, 740; ^{1}H NMR (400 MHz, DMSO-d_6, δ in ppm): 3.94 (s, 3H, NCH_3), 7.28 (t, 1H, J = 8.0 Hz, ArH), 7.42–7.78 (m, 7H, ArH and CH=CH), 7.86–8.06 (m, 6H, ArH

Table 2
Inhibition of tyrosinase, melanin production and cytotoxicity

Compound	L-tyrosine[a] IC_{50}(μM)	L-DOPA[a] IC_{50}(μM)	Melanin production Inhibition (%)	Cytotoxicity Cell viability (%)
7a	14.01 ± 3.12	15.15 ± 1.18	42.5 ± 0.43	86.7 ± 0.15
7b	>100	>100	9.7 ± 1.10	72.0 ± 1.21
7c	48.13 ± 4.12	56.45 ± 2.56	29.4 ± 2.15	80.5 ± 1.23
7d	17.52 ± 1.03	15.15 ± 0.43	36.1 ± 1.45	81.1 ± 2.56
7e	18.25 ± 2.16	15.18 ± 2.10	40.5 ± 2.65	84.5 ± 2.91
7f	35.16 ± 3.56	42.00 ± 2.12	20.6 ± 0.18	83.9 ± 1.43
7g	15.06 ± 1.59	16.54 ± 2.18	24.0 ± 0.78	88.7 ± 2.55
7h	>100	>100	10.2 ± 1.31	78.9 ± 2.82
7i	>100	>100	8.1 ± 2.02	60.9 ± 1.20
7j	35.16 ± 1.20	29.30 ± 0.18	21.7 ± 0.62	83.6 ± 1.55
7k	15.15 ± 3.25	15.18 ± 2.43	25.4 ± 1.52	82.7 ± 3.21
7l	>100	>100	11.6 ± 1.23	84.0 ± 1.40
7m	65.16 ± 4.26	75.02 ± 3.50	30.1 ± 2.35	80.1 ± 3.45
7n	46.53 ± 1.65	60.28 ± 2.10	10.7 ± 3.56	86.6 ± 5.64
7o	62.39 ± 2.65	71.92 ± 1.85	12.8 ± 5.12	82.1 ± 3.90
7p	85.15 ± 3.21	78.16 ± 2.65	15.9 ± 1.65	81.0 ± 2.85
7q	80.23 ± 4.60	74.45 ± 3.18	30.0 ± 0.85	79.5 ± 2.10
7r	80.15 ± 2.30	77.50 ± 1.30	15.6 ± 5.10	80.6 ± 2.65
8	48.15 ± 1.81	50.50 ± 1.10	20.1 ± 3.10	76.4 ± 1.90
Kojic Acid[b]	16.22 ± 1.74[c]	15.42 ± 1.40	16.1 ± 0.56[d]	80.0 ± 1.12[d]

[a] Values are the means of three experiments.
[b] Standard.
[c] Value in the literature is 16.3 μM[28].
[d] Tested at 200 μg/ml.

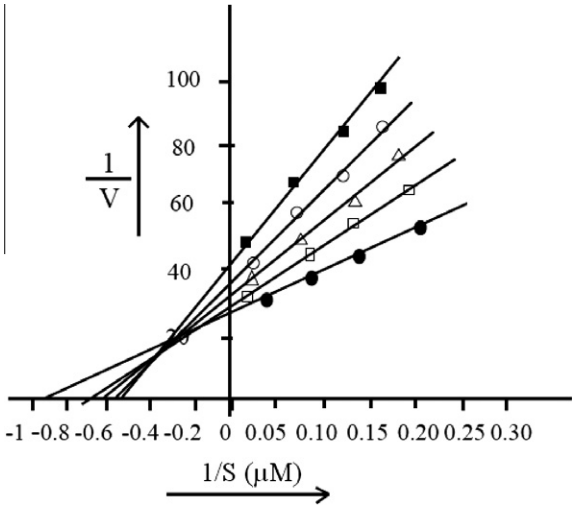

Figure 3. Lineweaver–Burk plot for the inhibition of compound **7a** on mushroom tyrosinase for catalysis of L-DOPA as a substrate. Concentrations of **7a** were 0 μM (●), 10 μM (□), 20 μM (Δ), 30 μM (o), 40 μM (■).

and CH=CH), 8.22 (d, 1H, *J* = 8.0 Hz, ArH), 8.41 (s, 1H, ArH), 8.77 (s, 1H, ArH), 10.75 (s, 1H, NH); *m*/*z* = 465.25 (m^+).

4.3.3. 3-Chloro-*N*-{3-[3-(9-methyl-9*H*-carbazol-3-yl)-acryloyl]-phenyl}-benzamide (7c)

Yield 85%; Mp: 142–145 °C; IR (KBr, cm^{-1}): 3315, 2984, 2870, 1652, 1622, 1615, 1538, 1507, 1438, 1009, 982, 867, 741; ^{1}H NMR (400 MHz, DMSO-d_6, δ in ppm): 3.94 (s, 3H, NCH_3), 7.29 (t, 1H, *J* = 8.0 Hz, ArH), 7.52 (t, 1H, *J* = 7.2 Hz, ArH), 7.60 (t, 2H, *J* = 7.6 Hz, ArH), 7.64 (d, 1H, *J* = 8.0 Hz, ArH), 7.69 (d, 2H, *J* = 8.8 Hz, ArH), 7.90 (d, 1H, *J* = 15.6 Hz, CH=CH), 7.94–8.05 (m, 4H, ArH and CH=CH), 8.08 (s, 1H, ArH), 8.14 (d, 1H, *J* = 8.0 Hz, ArH), 8.23 (d, 1H, *J* = 7.6 Hz, ArH), 8.45 (s, 1H, ArH), 8.75 (s, 1H, ArH), 10.59 (s, 1H, NH); *m*/*z* = 465.25 (m^+).

4.3.4. 4-Chloro-*N*-{3-[3-(9-methyl-9*H*-carbazol-3-yl)-acryloyl]-phenyl}-benzamide (7d)

Yield 87%; Mp: 248–250 °C; IR (KBr, cm^{-1}): 3310, 3185, 2980, 2874, 1622, 1650, 1530, 1507, 1438, 1005, 860; ^{1}H NMR (400 MHz, DMSO-d_6, δ in ppm): 3.92 (s, 3H, NCH_3), 7.28 (t, 1H, *J* = 7.2 and 8.0 Hz, ArH), 7.52 (t, 1H, *J* = 8.0 Hz, ArH), 7.59 (t, 1H, *J* = 7.6 Hz, ArH), 7.64 (d, 2H, *J* = 8.0 Hz, ArH), 7.69 (d, 1H, *J* = 8.4 Hz, ArH), 7.90 (d, 1H, *J* = 15.6 Hz, CH=CH), 7.95–8.06 (m, 6H, ArH and CH=CH), 8.13 (d, 1H, J = 8.0 Hz, ArH), 8.23 (d, 1H, *J* = 8.0 Hz, ArH), 8.44 (s, 1H, ArH), 8.74 (s, 1H, ArH), 10.53 (s, 1H, NH); *m*/*z* = 466.25 (m+1).

4.3.5. 2-Fluoro-*N*-{3-[3-(9-methyl-9*H*-carbazol-3-yl)-acryloyl]-phenyl}-benzamide (7e)

Yield 78%; Mp: 160–163 °C; IR (KBr, cm^{-1}): 3350, 3120, 2970, 1650,1620, 1580, 1468, 1407, 1009, 925, 740; ^{1}H NMR (400 MHz, DMSO-d_6, δ in ppm): 3.93 (s, 3H, NCH_3), 7.25–7.44 (m, 3H, ArH), 7.49–7.74 (m, 5H, ArH), 7.85–8.06 (m, 5H, ArH, CH=CH), 8.24 (d, 1H, *J* = 8.8 Hz, ArH), 8.33 (s, 1H, ArH), 8.41 (s, 1H, ArH), 8.74 (s, 1H, ArH), 10.64 (s, 1H, NH); *m*/*z* = 449.20 (m+1).

4.3.6. 3-Fluoro-*N*-{3-[3-(9-methyl-9*H*-carbazol-3-yl)-acryloyl]-phenyl}-benzamide (7f)

Yield 82%; Mp: 170–172 °C; IR (KBr, cm^{-1}): 3350, 3120, 2970, 1650,1620, 1580, 1468, 1407, 1009, 925, 816, 720; ^{1}H NMR (400 MHz, DMSO-d_6, δ in ppm): 3.92 (s, 3H, NCH_3), 7.28 (t, 1H, *J* = 8.0 Hz, ArH), 7.41–7.58 (m, 2H, ArH), 7.60–8.66 (m, 3H, ArH), 7.69 (d, 1H, J = 8.8 Hz, ArH), 7.82–7.90 (m, 2H, ArH, CH=CH), 7.92 (s, 1H, ArH), 7.94–8.06 (m, 3H, ArH, CH=CH), 8.14 (d, 1H, *J* = 8.0 Hz, ArH), 8.23 (d, 1H, *J* = 8.0 Hz, ArH), 8.44 (s, 1H, ArH), 8.75 (s, 1H, ArH), 10.59 (s, 1H, NH); *m*/*z* = 449.30 (m+1).

4.3.7. 4-Fluoro-*N*-{3-[3-(9-methyl-9*H*-carbazol-3-yl)-acryloyl]-phenyl}-benzamide (7g)

Yield 83%; Mp: 204–206 °C; IR (KBr, cm^{-1}): 3340, 2933, 2863, 1659, 1470, 1269, 1155, 1067, 777, 676; ^{1}H NMR (400 MHz, DMSO-d_6, δ in ppm): 3.94 (s, 3H, NCH_3), 7.27 (t, 1H, *J* = 8.0 Hz, ArH), 7.41 (t, 2H, *J* = 7.6 Hz, ArH), 7.52 (t, 1H, *J* = 8.0 Hz, ArH), 7.60 (t, 1H, *J* = 7.6 Hz, ArH), 7.65 (d, 1H, *J* = 8.0 Hz, ArH), 7.69 (d,

1H, *J* = 8.4 Hz, ArH), 7.90 (d, 1H, *J* = 15.6 Hz, CH=CH), 7.94–8.15 (m, 6H, ArH and CH=CH), 8.23 (d, 1H, *J* = 8.0 Hz, ArH), 8.43 (s, 1H, ArH), 8.75 (s, 1H, ArH), 10.54 (s, 1H, NH); *m*/*z* = 449.20 (m+1).

4.3.8. 3-Bromo-*N*-{3-[3-(9-methyl-9*H*-carbazol-3-yl)-acryloyl]-phenyl}-benzamide (7h)

Yield 81%; Mp: 119–122 °C; IR (KBr, cm^{-1}): 3297, 2926, 1654, 1560, 1464, 1433, 1205, 1105, 917, 805, 738; ^{1}H NMR (400 MHz, DMSO-d_6, δ in ppm): 3.94 (s, 3H, NCH_3), 7.29 (t, 1H, *J* = 7.6 Hz, ArH), 7.52 (t, 1H, *J* = 8.0 Hz, ArH), 7.60 (t, 2H, *J* = 7.6 Hz, ArH), 7.64 (d, 1H, *J* = 8.0 Hz, ArH), 7.70 (d, 2H, *J* = 8.8 Hz, ArH), 7.90 (d, 1H, *J* = 15.6 Hz, CH=CH), 7.95–8.06 (m, 4H, ArH and CH=CH), 8.10 (s, 1H, ArH), 8.14 (d, 1H, *J* = 8.0 Hz, ArH), 8.23 (d, 1H, *J* = 8.0 Hz, ArH), 8.44 (s, 1H, ArH), 8.76 (s, 1H, ArH), 10.59 (s, 1H, NH); *m*/*z* = 509 (m^+), 511.20 (m+2).

4.3.9. 2-Methyl-*N*-{3-[3-(9-methyl-9*H*-carbazol-3-yl)-acryloyl]-phenyl}-benzamide (7i)

Yield 80%; Mp: 150–152 °C; IR (KBr, cm^{-1}): 3294, 2931, 2845, 1655, 1590, 1460, 1318, 1257, 1205, 1106, 920, 806; ^{1}H NMR (400 MHz, DMSO-d_6, δ in ppm): 2.40 (s, 3H, CH_3), 3.92 (s, 3H, NCH_3), 7.28 (t, 1H, *J* = 8.0 Hz, ArH), 7.40–7.61 (m, 4H, ArH), 7.64 (d, 1H, *J* = 8.0 Hz, ArH), 7.70 (d, 1H, *J* = 15.2 Hz, CH=CH), 7.80–8.06 (m, 6H, ArH and CH=CH), 8.14 (d, 1H, *J* = 8.0 Hz, ArH), 8.23 (d, 1H, *J* = 8.0 Hz, ArH), 8.43 (s, 1H, ArH), 8.74 (s, 1H, ArH), 10.45 (s, 1H, NH); *m*/*z* = 445.30 (m+1).

4.3.10. 3-Methyl-*N*-{3-[3-(9-methyl-9*H*-carbazol-3-yl)-acryloyl]-phenyl}-benzamide (7j)

Yield 77%; Mp: 155–160 °C; IR (KBr, cm^{-1}): 3305, 2931, 2845, 1655, 1590, 1460, 1318, 1257, 1205, 1106, 920, 806, 738; ^{1}H NMR (400 MHz, DMSO-d_6, δ in ppm): 2.41 (s, 3H, CH_3), 3.92 (s, 3H, NCH_3), 7.27 (t, 1H, *J* = 8.0 Hz, ArH), 7.42 (s, 1H, ArH), 7.52 (t, 1H, *J* = 8.0, ArH), 7.59 (t, 1H, *J* = 8.4 Hz, ArH), 7.64 (d, 1H, *J* = 15.2 Hz, CH=CH), 7.70 (d, 1H, *J* = 15.2 Hz, CH=CH), 7.79–8.05 (m, 7H, ArH), 8.14 (d, 1H, *J* = 8.0 Hz, ArH), 8.24 (d, 1H, *J* = 8.0 Hz, ArH), 8.43 (s, 1H, ArH), 8.74 (s, 1H, ArH), 10.45 (s, 1H, NH); *m*/*z* = 445.30 (m+1).

4.3.11. 4-Methyl-*N*-{3-[3-(9-methyl-9*H*-carbazol-3-yl)-acryloyl]-phenyl}-benzamide (7k)

Yield 80%; Mp: 190–192 °C; IR (KBr, cm^{-1}): 3310, 3130, 2972, 1673, 1618, 1586, 1530, 1420, 1012, 925, 860; ^{1}H NMR (400 MHz, DMSO-d_6, δ in ppm): 2.40 (s, 3H, CH_3), 3.90 (s, 3H, NCH_3), 7.29 (t, 1H, *J* = 8.0 Hz, ArH), 7.52 (t, 1H, *J* = 8.0 Hz, ArH), 7.59 (t, 1H, *J* = 8.4 Hz, ArH), 7.63–7.68 (m, 3H, ArH and CH=CH), 7.69 (d, 1H, *J* = 8.4 Hz, ArH), 7.90 (d, 1H, *J* = 15.2 Hz, CH=CH), 7.98–8.05 (m, 5H, ArH), 8.13 (d, 1H, *J* = 8.0 Hz, ArH), 8.23 (d, 1H, *J* = 8.0 Hz, ArH), 8.44 (s, 1H, ArH), 8.74 (s, 1H, ArH), 10.50 (s, 1H, NH); *m*/*z* = 445.30 (m+1).

4.3.12. 4-*tert*-Butyl-*N*-{3-[3-(9-methyl-9*H*-carbazol-3-yl)-acryloyl]-phenyl}-benzamide (7l)

Yield 65%; Mp: 144–146 °C; IR (KBr, cm^{-1}): 3353, 3061, 2958, 1649, 1618, 1585, 1543, 1458, 1410, 1016, 918, 850, 761; ^{1}H NMR (400 MHz, DMSO-d_6, δ in ppm): 1.35 (s, 9H, $C(CH_3)_3$), 3.94 (s, 3H, NCH_3), 7.28 (t, 1H, *J* = 8.0 Hz, ArH), 7.50 (t, 1H, *J* = 8.0 Hz, ArH), 7.56–7.61 (m, 3H, ArH), 7.64 (d, 1H, *J* = 8.0 Hz, ArH), 7.69 (d, 1H, *J* = 8.4 Hz, ArH), 7.88–8.04 (m, 6H, ArH and CH=CH), 8.14 (d, 1H, *J* = 8.0 Hz, ArH), 8.23 (d, 1H, *J* = 8.0 Hz, ArH), 8.45 (s, 1H, ArH), 8.75 (s, 1H, ArH), 10.41 (s, 1H, NH); *m*/*z* = 487.40 (m+1).

4.3.13. *N*-{3-[3-(9-Methyl-9*H*-carbazol-3-yl)-acryloyl]-phenyl}-3-trifluoromethyl-benzamide (7m)

Yield 88%; Mp: 119–122 °C; IR (KBr, cm^{-1}): 3325, 3048, 2946, 2743, 1673, 1636, 1545, 1453, 1392, 1231, 1138, 1040, 894, 776; ^{1}H NMR (400 MHz, DMSO-d_6, δ in ppm): 3.93 (s, 3H, NCH_3), 7.29 (t, 1H, *J* = 7.6 Hz, ArH), 7.52 (t, 1H, *J* = 8.0 Hz, ArH), 7.56–7.65 (m, 3H, ArH), 7.70 (d, 2H, *J* = 8.4 Hz, ArH), 7.92 (d, 1H, *J* = 16 Hz, CH=CH), 7.95–8.06 (m, 4H, ArH and CH=CH), 8.08 (s, 1H, ArH), 8.14 (d, 1H, *J* = 8.4 Hz, ArH), 8.23 (d, 1H, *J* = 7.6 Hz, ArH), 8.44 (s, 1H, ArH), 8.75 (s, 1H, ArH), 10.59 (s, 1H, NH); *m*/*z* = 499.25 (m+1).

4.3.14. Furan-2-carboxylic acid {3-[3-(9-methyl-9*H*-carbazol-3-yl)-acryloyl]-phenyl}-amide (7n)

Yield 63%; Mp: 120–122 °C IR (KBr, cm^{-1}): 3306, 2923, 1656, 1592, 1467, 1319, 1204, 1105, 1108, 759, 589; ^{1}H NMR (400 MHz, DMSO-d_6, δ in ppm): 3.93 (s, 3H, NCH_3), 6.73 (m, 1H, ArH of furan), 7.28 (t, 1H, *J* = 8.0 Hz, ArH), 7.40 (m, 1H, ArH of furan), 7.52 (t, 1H, *J* = 8.0 Hz, ArH), 7.59 (t, 1H, *J* = 8.4 Hz), 7.64 (d, 1H, *J* = 15.2 Hz, CH=CH), 7.69 (d, 1H, *J* = 15.2 Hz, CH=CH), 7.82–8.06 (m, 5H, ArH and ArH of furan), 8.10 (d, 1H, *J* = 8.0 Hz, ArH), 8.22 (d, 1H, *J* = 8.0 Hz, ArH), 8.43 (s, 1H, ArH), 8.75 (s, 1H, ArH), 10.41 (s, 1H, NH); *m*/*z* = 421.30 (m+1).

4.3.15. Thiophene-2-carboxylic acid {3-[3-(9-methyl-9*H*-carbazol-3-yl)-acryloyl]-phenyl}-amide (7o)

Yield 60%; Mp: 90–93 °C; IR (KBr, cm^{-1}): 3315, 2924, 1650, 1590, 1432, 1317, 1205, 1105, 738; ^{1}H NMR (400 MHz, DMSO-d_6, δ in ppm): 3.93 (s, 3H, NCH_3), 7.28 (t, 1H, *J* = 8.0 Hz, ArH), 7.49–7.73 (m, 5H, ArH), 7.86–8.13 (m, 7H, ArH), 8.24 (d, 1H, *J* = 8.0 Hz, ArH), 8.38 (s, 1H, ArH), 8.76 (s, 1H, ArH), 10.47 (s, 1H, NH); *m*/*z* = 437.15 (m+1).

4.3.16. *N*-{3-[3-(9-Methyl-9*H*-carbazol-3-yl)-acryloyl]-phenyl}-3-phenyl-acrylamide (7p)

Yield 65%; Mp: 162–165 °C; IR (KBr, cm^{-1}): 3315, 2926, 1657, 1591, 1463,1257, 1106, 1013, 849, 760, 686; ^{1}H NMR (400 MHz, DMSO-d_6, δ in ppm): 3.91 (s, 3H, NCH_3), 6.84 (d, 1H, *J* = 16.0 Hz, CH=CH), 7.28 (t, 1H, *J* = and 8.0 Hz, ArH), 7.40–7.72 (m, 5H, ArH and CH=CH), 7.82–8.10 (m, 10H, ArH and CH=CH), 8.23 (d, 1H, *J* = 8.0 Hz, ArH), 8.38 (s, 1H, ArH), 8.74 (s, 1H, ArH), 10.45 (s, 1H, NH); *m*/*z* = 457.30 (m+1).

4.3.17. Cyclopropanecarboxylic acid {3-[3-(9-methyl-9*H*-carbazol-3-yl)-acryloyl]-phenyl}-amide (7q)

Yield 83%; Mp: 185–189 °C; IR (KBr, cm^{-1}): 3300, 2930, 1656, 1559, 1434, 1204, 1104, 1016, 955, 778, 688; ^{1}H NMR (400 MHz, DMSO-d_6, δ in ppm): 0.83 (m, 4H, cyclopropyl $(CH_2)_2$), 1.81 (m, 1H, cyclopropyl CH), 3.94 (s, 3H, NCH_3), 7.28 (t, 1H, *J* = 8.0 Hz, ArH), 7.58 (t, 2H, *J* = 8.0 Hz, ArH), 7.65 (d, 1H, *J* = 15.2 Hz, CH=CH), 7.70 (d, 1H, *J* = 15.2 Hz, CH=CH), 7.85–8.05 (m, 5H, ArH), 8.20–8.26 (m, 2H, ArH), 8.74 (s, 1H, ArH), 10.45 (s, 1H, NH); *m*/*z* = 395.25 (m+1).

4.3.18. *N*-{3-[3-(9-Methyl-9*H*-carbazol-3-yl)-acryloyl]-phenyl}-acetamide (7r)

Yield 88%; Mp: 160–164 °C; IR (KBr, cm^{-1}): 3300, 2930, 1656, 1559, 1434, 1204, 1104, 1016, 955, 778, 688; ^{1}H NMR (400 MHz, DMSO-d_6, δ in ppm): 2.09 (s, 3H, CH_3), 3.94 (s, 3H, NCH_3), 7.28 (t, 1H, *J* = 8.0 Hz, ArH), 7.58 (t, 2H, *J* = 8.0 Hz, ArH), 7.65 (d, 1H, *J* = 15.2 Hz, CH=CH), 7.70 (d, 1H, *J* = 15.2 Hz, CH=CH), 7.85–8.05 (m, 5H, ArH), 8.20–8.26 (m, 2H, ArH), 8.73 (s, 1H, ArH), 10.17 (s, 1H, NH); *m*/*z* = 369.20 (m+1).

4.4. Synthesis of (*E*)-1-(3-aminophenyl)-3-(9-methyl-9*H*-carbazol-3-yl)-prop-2-en-1-one (8)

3-Aminoacetophenone **4** (1 mmol) was dissolved in ethanol (15 ml), 1 ml 20% NaOH solution was added to it and stirred for 10 min at room temperature. Then, 3-formyl-9-methylcarbazole **3** (1 mmol) was added and stirring continued for 24 h at room

temperature. After completion of reaction (TLC), reaction mixture was poured over crushed ice and stirred. The precipitate obtained was filtered and recrystallized by using methanol to obtain the target compound **8**. Yield: 70%; Yellow solid; Mp: 112–116 °C; IR (KBr, cm^{-1}): 3415, 3320, 2930, 1656, 1559, 1434, 1204, 1104, 1016, 955, 778; ^1H NMR (400 MHz, DMSO-d_6, δ in ppm): 3.93 (s, 3H, NCH_3), 5.36 (s, 2H, NH_2), 7.24 (t, 1H, J = 8.0 Hz, ArH), 7.49–7.90 (m, 5H, ArH), 8.01–8.31 (m, 4H, ArH and CH=CH), 7.75 (d, 1H, J = 15.9 Hz, CH=CH), 8.79 (s, 1H, ArH), 8.86 (s, 1H, ArH); m/z = 327.20 (m+1).

4.5. Biology

4.5.1. Xanthine oxidase (XO) assay

Bovine milk XO (grade 1, ammonium sulfate suspension, Sigma–Aldrich) activity was assayed spectrophotometrically by measuring the uric acid formation at 293 nm using a UV–visible spectrophotometer at 25 °C.[29] The reaction mixture contained 50 mM potassium phosphate buffer (pH 7.6), 75 μM xanthine and 0.08 units of XO. Inhibition of XO activity by various inhibitors was measured by following the decrease in the uric acid formation at 293 nM at 25 °C. The enzyme was preincubated for 5 min, with test compound, dissolved in DMSO (1% v/v), and the reaction was started by the addition of xanthine. Final concentration of DMSO (1% v/v) did not interfere with the enzyme activity. All the experiments were performed in triplicate and values were expressed as means of three experiments.

4.5.2. Molecular modelling

The active site prediction and determination of the active site residues of Xanthine oxidase (1fiq) was done by automatic sequence alignment mode in Accelrys Drug Discovery suite. Active site was located by selecting cocrystalized ligand 2-hydroxy benzoic acid in XO, embedded in a 5 Å shell of residues, water and HETs (hetero atoms) and saved as active site pocket. In this study, 19 newly synthesized carbazole derivatives were evaluated for their in silico interactions with XO. The ligands were selected and refined for lowest energy rotamer by molecular mechanics procedure in Accelrys. The ligands were then docked over the enzymes active site. Program automates the docking of ligand into the active site using a genetic algorithm with a fast, simplified potential of meanforce (PMF).[30] PMF has been demonstrated to show a significant correlation between experimental binding affinities and its computed score for diverse protein–ligand complexes.[31–35] The models of ligands with enzymes active site were build using the graphical user interface by MacroModel (Maestro GUI), and a 1000 iteration step MonteCarlo simulation was carried out randomizing all rotatable bonds. Each conformation was energy minimized with the force field AMBER united atom and the GB/SA water implicit model of solvation and deduplicated according to a root-mean square deviation (RMSD) in the atomic coordinates and an energy difference respectively lower than 0.25 and 1 kcal/mol. The Protein Data Bank crystallographic structures of enzyme were considered for docking experiments. The models were then refined by means of potential energy minimization using the AMBER force field implemented in MacroModel ver. 7.2. The flexible docking experiments were carried out with the Accelrys software. The binding sites were obtained by manual positioning of the global minimum energy of the carbazole derivatives.

4.5.3. Tyrosinase assay

The inhibitory effect of target compounds on tyrosinase activity was carried out according to the procedure by Khatib et.al.[36] with some modification. Equal volume of phosphate buffer (50 mM, pH 6.8) and 333 units/ml of tyrosinase (SIGMA) was added into 96-well microtiter plate. The test samples dissolved in DMSO were then added into each well. After 5 min incubation, L-tyrosine/L-DOPA (0.5 mM) was added and the absorbance was measured at 492 nm for 1 min. The measurements were performed in triplicate for each concentration of test sample.

4.5.4. Melanin production inhibition

Melanin production inhibition was determined by previously described method by Wang et. al.[37] with minor modifications. On day 1, a total of 8×10^4 cells were added to 60 mm plates, and incubated at 37 °C in a CO_2 incubator. On day 2, 10 μl test samples in DMSO were added to plates and incubated for 72 h at 37 °C in a CO_2 incubator. After washing with PBS, cells were lysed with 1 ml of 1 N NaOH, and 200 μl portions of crude cell extracts were transferred to 96-well plates. Melanin production inhibition was determined by recording absorbance at 475 nm. The effects of test samples on melanin contents are expressed as percent inhibitions of the value obtained in B16F10 mouse melanoma cells cultured with DMSO alone (control).

4.5.5. Cytotoxicity assay (MTT assay)

MTT assays were performed using a micro-culture MTT method described by Han et. al.[38] A B16F10 mouse melanoma cell suspension was poured into a 96-well plate (10^3 cells/well) and cells were allowed to completely adhere overnight. Test samples were then added to the plate and incubated at 37 °C for 72 h in a CO_2 incubator. 20 μl of MTT solution (2 mg/ml) was then added per well and incubated for 4 h. Supernatant was then removed and formazan was solubilised by adding 150 μl DMSO to each well with gentle shaking. Absorbance at 490 nm was recorded using an ELISA plate reader.

Acknowledgement

H.V.C. grateful to Council of Scientific and Industrial Research (CSIR), New Delhi, India for financial assistance in the form of SRF.

Supplementary data

Supplementary data associated with this article can be found, in the online version, at http://dx.doi.org/10.1016/j.bmc.2012.07.001.

References and notes

1. Harris, M. D.; Siegel, L. B.; Alloway, J. A. *Am. Fam. Physician.* **1999**, *59*, 925.
2. Droge, W. *Physiolo. Rev.* **2002**, *82*, 47.
3. Wijk, R. V.; Wijk, E. P. A. V.; Wiegant, F. A. C.; Ives, J. I. *J. Exp. Biol.* **2008**, *46*, 273.
4. Tomita, M.; Mizuno, S.; Yamnaka, H.; Hosoda, Y.; Sakuma, K.; Matuoka, Y.; Odaka, M.; Yamaguchi, M.; Yosida, H.; Morisawa, H.; Murayama, T. *J. Epidemical.* **2000**, *10*, 403.
5. Nakayawa, T.; Hu, H.; Zharkov, S.; Tuttle, K. R.; Short, R. A.; Glushakova, O.; Ouyang, X.; Feig, D. I.; Block, E. R.; Herrera-Acosta, J.; Patel, J. M.; Johnson, R. J. *Am. J. Physiol. Renal Physiol.* **2006**, *290*, 625.
6. Naeff, H. S. D.; Franssen, M. C. R.; Van der Plas, H. C. *Recl. Trav. Pays-Bas.* **1991**, *11*, 139.
7. Murata, K.; Nakao, K.; Hirata, N.; Namba, K.; Nomi, T.; Kitamura, Y.; Moriyama, K.; Shintani, T.; Linuma, M.; Mastuda, H. *J. Nat. Med.* **2009**, *63*, 355.
8. Hande, K. R.; Noone, R. M.; Stone, W. J. *Am. J. Med.* **1984**, *76*, 47.
9. Reinders, M. K.; Jansen, T. L. T. A. *Clin. Interv. Aging.* **2010**, *5*, 7.
10. Okamoto, K.; Matsumoto, K.; Hille, R.; Eger, B. J.; Pai, E. F.; Nishino, T. *Proc. Natl. Acad. Sci. U.S.A.* **2004**, *101*, 7931.
11. Ishibuchi, S.; Morimoto, H.; Oe, T.; Ikebe, T.; Inoue, H.; Fukunari, A.; Kamezawa, M.; Yamada, I.; Naka, Y. *Bioorg. Med. Chem. Lett.* **2001**, *11*, 879.
12. Lin, C. M.; Chen, C. S.; Chen, C. T.; Liang, Y. C.; Lin, J. K. *Biochem. Biophys. Res. Commun.* **2002**, *294*, 167.
13. Niu, Y.; Zhu, H.; Liu, J.; Fan, H.; Sun, L.; Lu, W.; Liu, X.; Li, L. *Chem. Biol. Inter.* **2011**, *189*, 161.
14. Nepali, K.; Singh, G.; Tarun, A.; Agarwal, A.; Sapra, S.; Kumar, R.; Banerjee, U. C.; Verma, P. K.; Suri, O. P.; Dhar, K. L. *Bioorg. Med. Chem.* **2011**, *19*, 1950.
15. Nepali, K.; Agarwal, A.; Sapra, S.; Mittal, V.; Kumar, R.; Banerjee, U. C.; Gupta, M. K.; Satii, N. K.; Suri, O. P.; Dhar, K. L. *Bioorg. Med. Chem.* **2011**, *19*, 5569.
16. Pauff, J. M.; Hille, R. *J. Nat. Prod.* **2009**, *72*, 725.
17. (a) Ando, H.; Kondoh, H.; Ichihashi, M.; Hearing, V. J. *J. Invest. Dermatol.* **2007**, *127*, 751; (b) Wang, H. M.; Chen, C. Y.; Wen, Z. H. *Exp. Dermatol.* **2010**, *20*, 242.

18. Ito, S. *Pigment Cell Res.* **2003**, *16*, 230.
19. Raper, H. S. *Physiolo. Rev.* **1928**, *8*, 245.
20. Asanuma, A.; Miyazaki, I.; Ogawa, N. *Neurofox. Res.* **2003**, *5*, 165.
21. Martinez, M. V.; Whitaker, J. R. *Trends Food Sci. Tech.* **1995**, *6*, 195.
22. Knolker, H. J.; Reddy, K. R. *Chem. Rev.* **2002**, *102*, 4303.
23. Noguchi, N.; Nishino, K.; Niki, E. *Biochem. Pharmacol.* **2000**, *59*, 1069.
24. Zall, A.; Kieser, D.; Hottecke, N.; Naumann, E. C.; Thomaszewski, B.; Schneider, K.; Steinbacher, D. T.; Schubenel, R.; Masur, S.; Baumann, K.; Schmidt, B. *Bioorg. Med. Chem.* **2011**, *19*, 4903.
25. Routier, S.; Merour, J. Y.; Dias, N.; Lansiaux, N.; Bailly, C.; Lozach, O.; Meijer, L. *J. Med. Chem.* **2006**, *49*, 789.
26. Hu, L.; Li, Y. R.; Li, Y.; Qu, J.; Ling, Y. H.; Jiang, J. D.; Boykin, D. W. *J. Med. Chem.* **2006**, *49*, 6273.
27. Bandgar, B. P.; Sarangdhar, R. J.; Viswakarma, S.; Ali Ahamed, F. *J. Med. Chem.* **2011**, *54*, 1191.
28. Cho, S. J.; Roh, J. S.; Sun, W. S.; Kim, S. H.; Park, K. D. *Bioorg. Med. Chem. Lett.* **2006**, *16*, 2682.
29. Takano, Y.; Hase-Aoki, K.; Horiuchi, H.; Zhao, L.; Kasahara, Y.; Kondo, S.; Becker, M. A. *Life Sci.* **2005**, *76*, 1835.
30. Muegge, I.; Mrtin, Y. C. *J. Med. Chem.* **1999**, *42*, 791.
31. Muegge, I. *Med. Chem. Res.* **1998**, *9*, 490.
32. Muegge, I.; Martin, Y.; Hajduk, P. J.; Fesik, S. W. *J. Med. Chem.* **1999**, *42*, 2498.
33. Ha, S.; Andreani, R.; Robbins, A.; Muegge, I. *Comput. Aided Mol. Des.* **2000**, *14*, 435.
34. Muegge, I.; Rarey, M. *Rev. Comput. Chem.* **2001**, *17*, 1.
35. Cornell, W. D.; Cieplak, P.; Bayly, C. I.; Gould, I. R.; Merz, K. M., Jr.; Forguson, D. M.; Spellmeyer, D. C.; Fox, T.; Caldwell, J. W.; Kollman, P. A. *J. Am. Chem. Soc.* **1995**, *117*, 5179.
36. Khatib, S.; Nerya, O.; Musa, R.; Shmuel, M.; Tamir, S.; Vaya, J. *Bioorg. Med. Chem.* **2005**, *13*, 433.
37. Wang, H. M.; Chen, C. Yi.; Chen, C. Y.; Ho, M. L.; Chou, Y. T.; Chang, H. C.; Lee, C. H.; Wang, C. Z.; Chu, I. M. *Bioorg. Med. Chem.* **2010**, *18*, 5241.
38. Han, J.; Ma, I.; Hendzel, M. J.; Turner, J. A. *Breast Cancer Res.* **2009**, *11*, R57.